

Supplementary Information

Applied Microbiology and Biotechnology

Functional and structural insights into a thermostable (S)-selective amine transaminase and its improved substrate scope by protein engineering

Stefania Patti^{1,2#}, Simone A. De Rose^{3#}, Michail N. Isupov³, Ilaria Magrini Alunno¹, Sergio Riva¹, Erica Elisa Ferrandi^{1*}, Jennifer A. Littlechild^{3*}, Daniela Monti^{1*}

¹ Istituto di Scienze e Tecnologie Chimiche “G. Natta” (SCITEC), CNR, Milano, Italy

² Department of Pharmaceutical Sciences, University of Milan, Milano, Italy

³ Henry Wellcome Building for Biocatalysis, Biosciences, Faculty of Health and Life Sciences, University of Exeter, Exeter, United Kingdom

These authors contributed equally to this work

*Corresponding authors

Email - Jennifer A. Littlechild, J.A.Littlechild@exeter.ac.uk; Erica Elisa Ferrandi, erica.ferrandi@scitec.cnr.it; Daniela Monti, daniela.monti@scitec.cnr.it

Index

Site-directed mutagenesis	p. 2
Table S1. Primers used in this study	p. 3
Table S2. Mutants expression yields	p. 3
Table S3. Sbv333-ATA stability to water-miscible co-solvents	p. 4
Table S4. Sbv333-ATA stability in biphasic systems (1:1)	p. 4
Table S5. Amine donor screening with wild-type Sbv333-ATA and engineered variants.	p. 5
Table S6. Detailed crystallization conditions for all the Sbv333-ATA structures	p. 6
Figure S1. Chemical structure of the substrate phenylacetylcarbinol (PAC) and the product analogue norephedrine tested in Sbv333-ATA co-crystallization experiments.	p. 6
Figure S2. Chemical structure of aromatic (R)-amines with increasing side-chain lengths tested as substrates with Sbv333-ATA variants	p. 6
Figure S3. Screening of Sbv333-TA mutants designed for reverse enantioselectivity.	p. 7
Figure S4. Deamination of selected aromatic (R)-amines catalyzed by W89A Sbv333-ATA variant at different pH values.	p. 7
Figure S5. Transaminase amino acid structural alignments of the active site area of Sbv333-ATA, <i>Silicibacter</i> sp. tm1040 (PDB: 3FCR), <i>Silicibacter pomeroyi</i> (PDB: 3HMU) and <i>Vibrio fluvialis</i> (PDB: 4E3Q).	p. 8
Figure S6: Schematic overview of stabilising interactions of the Sbv333 gabaculine complex.	p. 9
References	p. 9

Site-directed mutagenesis

Sbv333-TA variants carrying up to two-point mutations were created by a Q5[®] Site-Directed Mutagenesis Kit (New England BioLabs) and a QuikChange II XL site-directed mutagenesis kit (Agilent) according to the manufacturer's protocols. Mutagenesis primers (Table S1) were designed using the primer design program suggested by the respective manufacturer (<https://international.neb.com/tools-and-resources/video-library/nebasechanger-designing-primers-for-use-with-the-q5-site-directed-mutagenesis-kit>; <https://www.agilent.com/store/primerDesignProgram.jsp>).

A typical PCR mixture (25 μ L) for the Q5[®] Site-Directed Mutagenesis Kit consisted of 12.5 μ L of Q5 Hot Start High-Fidelity 2X Master Mix, 1.25 μ L of 10 μ M Forward Primer, 1.25 μ L of 10 μ M Reverse Primer; 1-25 ng of Template DNA and 9 μ L of Nuclease-free Water. After initial denaturation for 30 sec at 98 $^{\circ}$ C, the cycling program was followed for 25 cycles: 10 sec, 98 $^{\circ}$ C, denaturation; 10-30 sec, primer annealing at the primer specific optimal annealing temperature; and 20-30 sec/kb, 72 $^{\circ}$ C. elongation. The final extension step was performed for 2 min at 72 $^{\circ}$ C. After PCR, the amplified material is added directly to a Kinase-Ligase-DpnI (KLD) enzyme mix for rapid, room temperature circularization and template removal. The mixture is composed by: 1 μ L of PCR product; 5 μ L of 2X KLD Reaction Buffer; 1 μ L of 10X KLD enzyme mix and 3 μ L of Nuclease-free Water. The mixture was then incubated at room temperature for 5 min, then transformation into NEB 5-alpha Competent *E. coli* cells was performed. Clones from an overnight growth on agar plates supplemented with kanamycin were inoculated in a 5 mL overnight cultivation (LB media, kanamycin complemented). Plasmids were isolated from the overnight culture using GeneJET Plasmid Miniprep Kit (Thermo Scientific[™]). To verify the presence of the single point mutation plasmids were sequenced by Eurofins (UK).

A typical PCR mixture (50 μ L) for the QuikChange II XL site-directed mutagenesis kit consisted of 5 μ L of 10x reaction buffer (12.5 μ L), 1 μ L of a mixture of deoxynucleoside triphosphates, 3 μ L of QuickSolution, 1 μ L of *PfuTurbo* DNA polymerase (2.5 U/ μ L), 10 ng of plasmid DNA and the forward and reverse primers (0.5 μ M) and ddH₂O to a final volume of 50 μ L. After initial denaturation for 1 min at 95 $^{\circ}$ C, the cycling program was followed for 18 cycles: 50 sec, 95 $^{\circ}$ C, denaturation; 50 sec, primer annealing at the primer specific optimal annealing temperature; and 1 min/kb (4 min), 68 $^{\circ}$ C, elongation. The final elongation step was performed for 7 min at 68 $^{\circ}$ C. After PCR, the reaction mixtures were digested for 1 h at 37 $^{\circ}$ C with *Dpn* I (10 U/ μ L), followed by transformation into XL10-Gold ultracompetent cells. Clones from an overnight growth on agar plates supplemented with kanamycin were used for inoculation of a 5 mL overnight cultivation (LB media, kanamycin complemented). Plasmids were isolated from the overnight culture using HiSpeed[®] Plasmid Midi Kit (Qiagen, Hilden, Germania). To verify the presence of the single point mutation plasmids were sequenced by Bio-Fab Research (Rome).

Table S1. Primers used in this study

Position and mutation	Primer Sequence
F61A (forward)	GGCGGGCCTCgcgGTCGTGCAGG
F61A (reverse)	AGTCCGTCCAGGTACCGC
W89A (forward)	CTTCCCATCgcgTCGTACGCCACC
W89A (reverse)	AAGGCCAGGTCTGTGCC
L60A (forward)	ACTGGCGGGCgcgTTCGTGTGCAGGCC
L60A (reverse)	CCGTCCAGGTACCGCCG
W89Y (forward)	CTTCCCATCtacTCGTACGCCACCC
W89Y (reverse)	AAGGCCAGGTCTGTGCC
F61C (forward)	CTGCACGACgcaGAGGCCCGCCAGTC
F61C (reverse)	GACTGGCGGGCCTCtgcGTCGTGCAG
F61V (forward)	CCTGCACGACgacGAGGCCCGCCAG
F61V (reverse)	CTGGCGGGCCTCgtcGTCGTGCAGG
F23V (forward)	CGACATGCGCGTgacGTGCATCCACAGGT
F23V (reverse)	ACCTGTGGATGCACgtcACGCGCATGTCG
L60V (forward)	GCACGACGAagacGCCCGCCAGTCC
L60V (reverse)	GGACTGGCGGGCgtcTTCGTGTGC
F23W (forward)	GACATGCGCGTccaGTGCATCCACAGGTGGTTCGT
F23W (reverse)	ACGACCACCTGTGGATGCACtggACGCGCATGTC
D421E (forward)	CGCCGCGGTcctcGGCGCGGC
D421E (reverse)	GCCGCGCCgagGACCGCGGCG
D421W (forward)	GGTCGCCGCGGTccaGGCGCGGCAGTAG
D421W (reverse)	CTACTGCCGCGCctggGACCGCGGCGACC
F61W (forward)	CGGCCTGCACGACccaGAGGCCCGCCAG
F61W (reverse)	CTGGCGGGCCTCtggGTCGTGCAGGCCG

For heterologous protein production, the isolated plasmids were transformed into *E. coli* BL21(DE3) cells containing plasmid pGRO7 (Takara Bio Inc., Kyoto, Japan) coding for co-chaperons GroES and GroEL. Protein expression yields are reported in Table S2.

Table S2. Mutants expression yields

Mutation	Protein expression yield (mg L _{culture} ⁻¹)
F23V	99
L60A	-
L60V	56
F61A	-
F61V	119
F61C	99
W89A	54
W89Y	-
Y153W	38
W89Y/ Y153W	66
W89A/ F23W	-
W89A/ F61W	68
W89A/ D421E	82
W89A/ D421W	97

- **Sbv333-TA functional characterization**

Table S3. Sbv333-ATA stability to water-miscible co-solvents

Time (h)	Co-solvents	U mL ⁻¹	Residual activity (%)
0	None	1.34	100
5		1.38	103
24		0.73	54
0	MeOH 5%	1.11	100
5		0.95	86
24		0.62	56
0	MeOH 10%	1.11	100
5		1.23	111
24		0.73	66
0	MeOH 20%	0.98	100
5		1.08	110
24		0.63	64
0	EtOH 5%	1.29	100
5		1.29	100
24		0.51	40
0	EtOH 10%	1.24	100
5		1.27	102
24		0.57	46
0	EtOH 20%	1.05	100
5		1.37	109
24		0.56	53
0	ACN 5%	1.16	100
5		1.08	93
24		1.02	88
0	ACN 10%	1.16	100
5		1.20	103
24		0.77	66
0	ACN 20%	1.14	100
5		1.28	112
24		0.76	67
0	DMSO 5%	1.20	100
5		1.31	109
24		1.10	92
0	DMSO 10%	1.28	100
5		1.33	104
24		1.06	83
0	DMSO 20%	1.30	100
5		1.06	82
24		1.00	77

Table S4. Sbv333-ATA stability in biphasic systems (1:1)

Time (h)	Solvents	U mL ⁻¹	Residual activity (%)
0	None	1.00	100
5		0.95	95
24		0.65	65
5	PE	0.95	95
24		0.51	51
5	Tol	1.12	112
24		0.71	71
5	EtOAc	1.19	109
24		0.68	68

Table S5. Amine donor screening with wild-type Sbv333-ATA and engineered variants.

Enzyme	Substrate	$\Delta mAbs \text{ min}^{-1}$	$mU \text{ mL}^{-1}$	$mg \text{ mL}^{-1}$	$mU \text{ mg}^{-1}$
WT	(S)-1	12.49	375.64	11.5	32.66
	(S)-5	12.49	375.64		32.66
	7	1.66	49.92		4.34
	10	1.92	57.62		5.01
	11	21.45	645.11		56.10
	12	15.88	477.59		41.53
	15	3.40	102.17		8.88
	(S)-20	7.99	240.57		20.92
	21	7.86	236.24	20.54	
F23V	(S)-5	0.61	18.22	16	1.14
	11	1.29	38.83		2.43
L60V	(S)-1	0.33	10.03	7.4	1.36
	10	0.13	4.00		0.54
	12	0.41	12.47		1.69
	19	0.13	4.14		0.56
F61C	(S)-1	20.46	615.34	19.9	30.92
	(S)-3	1.25	37.71		1.90
	(S)-5	22.98	691.13		34.73
	7	3.47	104.39		5.25
	10	2.47	74.17		3.73
	11	10.83	325.71		16.37
	12	23.16	696.54		35.00
	15	6.97	209.65		10.54
	(S)-20	7.81	234.86		11.80
	21	6.46	194.20		9.76
W89A	(S)-1	3.35	100.78	12	8.40
	(S)-3	2.17	65.32		5.44
	4	7.31	219.76		18.31
	(S)-5	4.54	136.51		11.38
	7	2.80	84.06		7.01
	10	0.19	5.69		0.47
	11	17.32	520.90		43.41
	12	15.91	478.50		39.87
	15	2.77	83.16		6.93
	21	2.99	90.20		7.52
W89A/L60V	(S)-1	0.22	6.70	9.52	0.70
	(S)-3	0.51	15.32		1.61
	(S)-5	0.34	10.27		1.08
	7	0.14	4.19		0.44
	10	0.29	8.82		0.93
	11	1.20	36.21		3.80
	19	0.17	5.18		0.54

Table S6. Detailed crystallization conditions for all the Sbv333-ATA structures

Sbv333-ATA	Crystallization conditions
Native	0.2 M potassium thiocyanate; 0.1 M Bis Tris propane 6.5; 20 % w/v PEG 3350
Gabaculine	10 mM Gabaculine 0.2 M potassium thiocyanate 0.1 M Bis Tris propane 6.5 20 % w/v PEG 3350
Phenylacetylcarbinol (PAC)	10 mM PAC; 0.1 Imidazole; MES monohydrate (acid) pH 6.5; 30% Precipitant mix (40% v/v (PEG 500* MME; 20 % w/v PEG 20000); Additives: 0.2M D-Glucose; 0.2M D-Mannose; 0.2M DGalactose; 0.2M L-Fucose; 0.2M D-Xylose; 0.2M N-Acetyl-D-Glucosamine
Norephedrine	10 mM 1s2s Pseudoephedrine; 0.1 M Bis-Tris propane, pH 6.5; 20 % w/v PEG 3350; 0.2 M Sodium iodide
W89A	0.3M Diethylene glycol; 0.3M Triethylene glycol; 0.3M Tetraethylene glycol; 0.3M Pentaethylene glycol; Tris (base) BICINE pH 8.5; 30% Precipitant mix (40% v/v PEG 500* MME; 20% w/v PEG 20000)
F61C	0.2 M Magnesium chloride hexahydrate; 0.1 M Tris 7.5; 25 % w/v PEG 2000 MME

Figure S1. Chemical structure of the substrate phenylacetylcarbinol (PAC) and the product analogue norephedrine tested in Sbv333-ATA co-crystallization experiments.

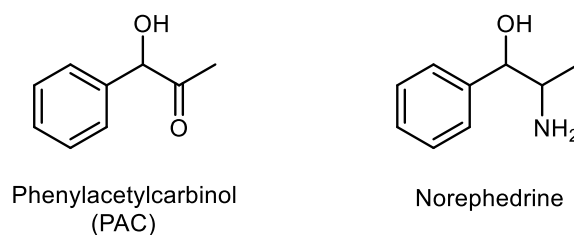


Figure S2. Chemical structure of aromatic (*R*)-amines with increasing side-chain lengths tested as substrates with Sbv333-ATA variants.

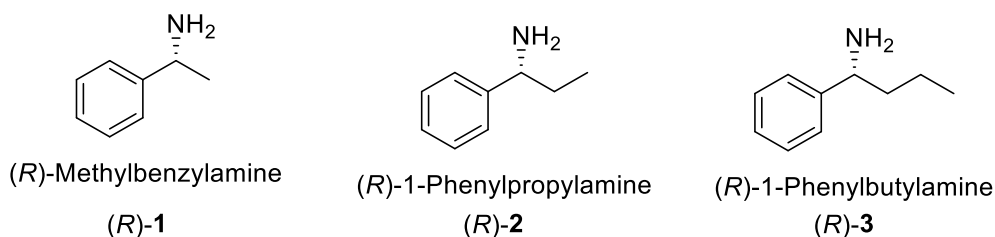


Figure S3. Screening of Sbv333-TA mutants designed for reverse enantioselectivity.

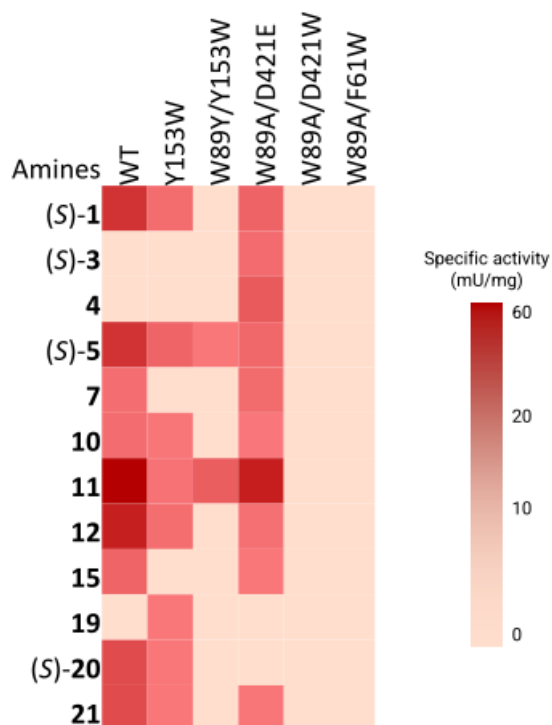


Figure S4. Deamination of selected aromatic (*R*)-amines catalyzed by W89A Sbv333-ATA variant at different pH values.

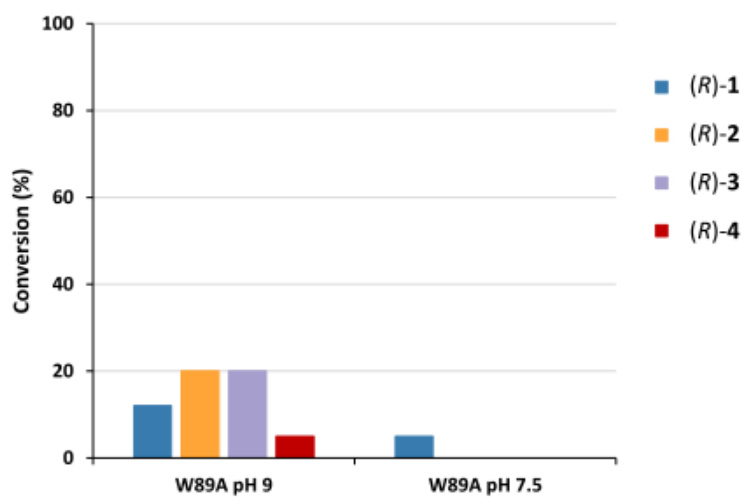
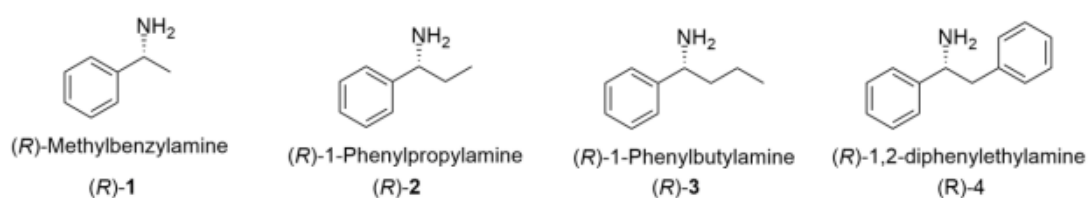
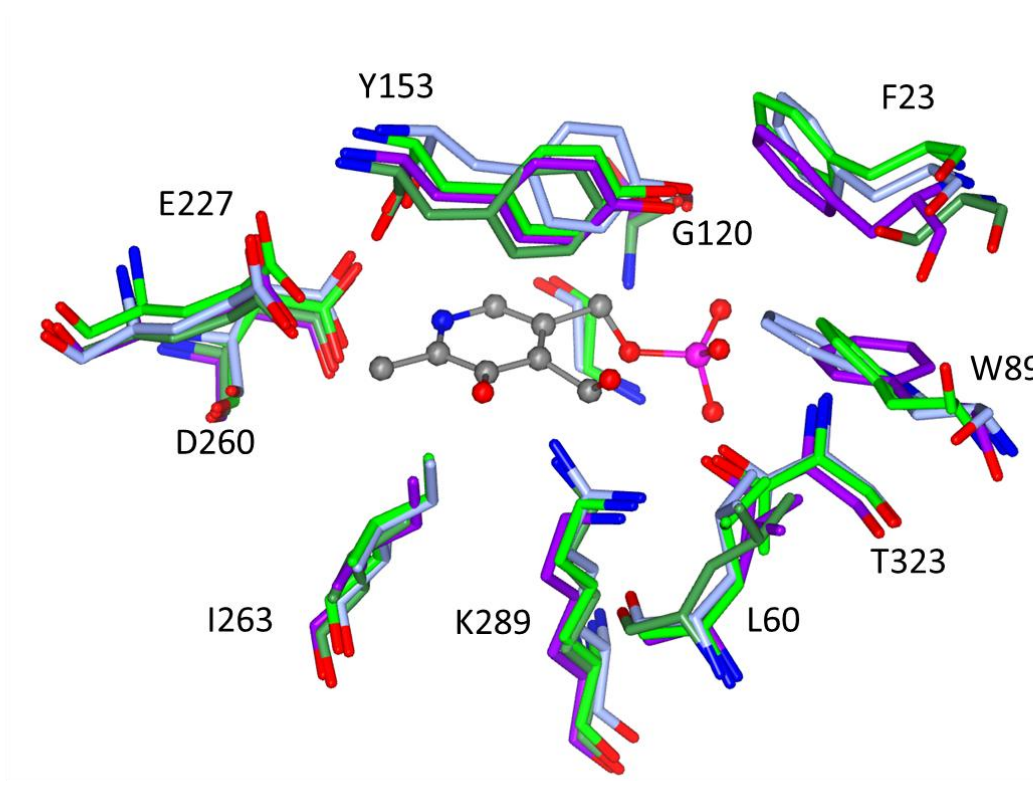
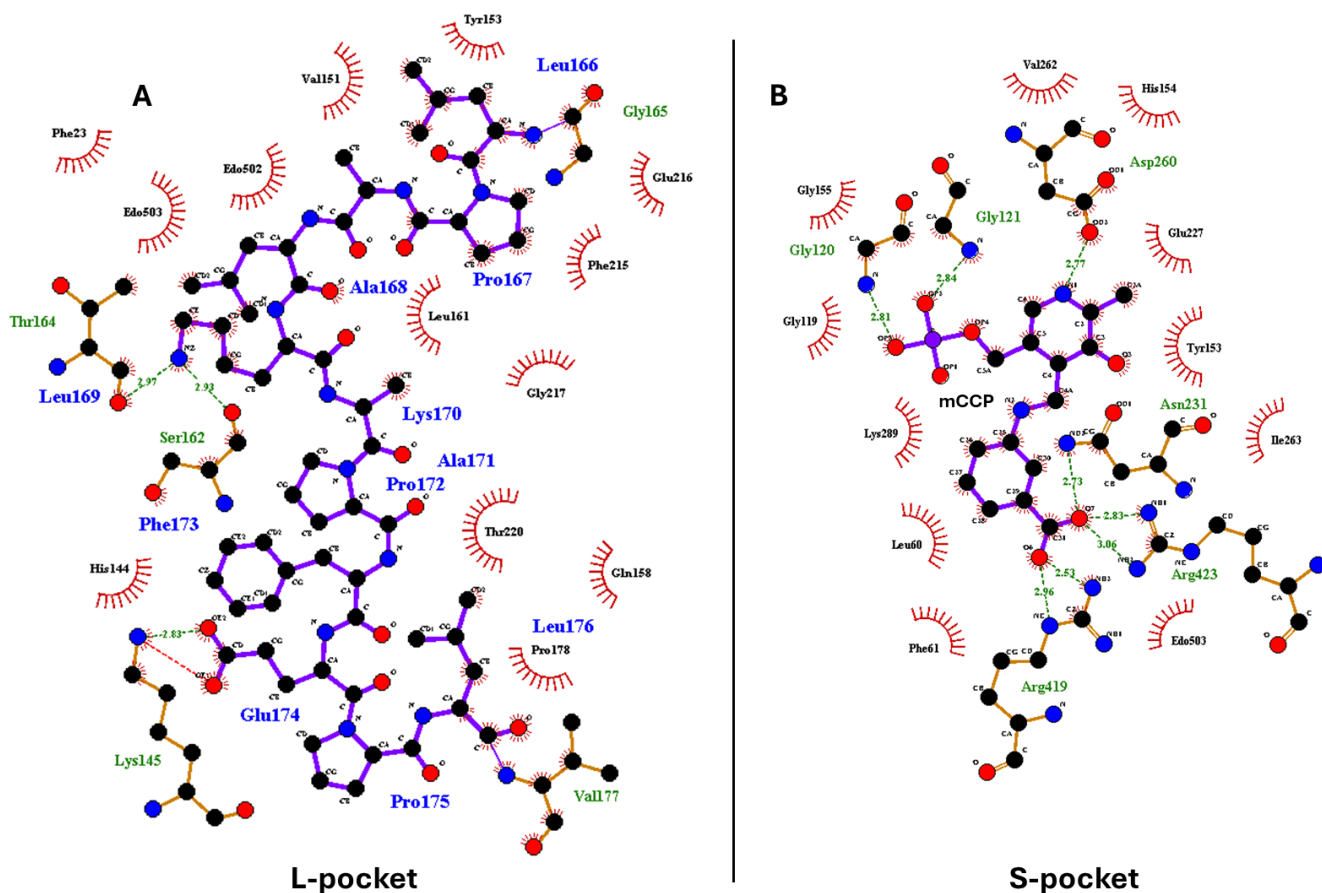


Figure S5. Transaminase amino acid structural alignments of the active site area of Sbv333-ATA, *Silicibacter sp.* tm1040 (PDB: 3FCR), *Silicibacter pomeroyi* (PDB: 3HMU) and *Vibrio fluvialis* (PDB: 4E3Q). The proteins Sbv333-ATA, 3FCR, 3HMU and 4E3Q are shown as cyan, green, yellow and purple sticks, respectively. The oxygen and nitrogen atoms of different residues are coloured red and blue, PLP is shown as a grey ball and stick model.



Sbv333	F23	L60	W89	G120	Y153	E227	D260	I263	K289	T323
3FCR	S19	L58	Y87	S120	Y152	E226	D259	V262	K288	T325
3HMU	F25	L62	F91	G123	Y156	E228	D261	I264	K290	T322
4E3Q	F19	L56	F85	S118	Y150	E223	D256	I259	K285	T322

Figure S6: Schematic overview of stabilising interactions of the Sbv333 gabaculine complex. **(A)** a portion of the large pocket showing the residue range from L166 to L176. **(B)** The small pocket with all the residues and the gabaculine molecule shown. Hydrogen bonds are shown as green dashes and their distances indicated. Residues involved in hydrophobic interaction are shown as red radiated semicircle. Figure generated using LigPlot+ (Wallace et al. 1995; Laskowski and Swindells 2011).



References

- Laskowski RA, Swindells MB (2011) LigPlot+: Multiple Ligand–Protein Interaction Diagrams for Drug Discovery. *J Chem Inf Model* 51:2778–2786. <https://doi.org/10.1021/ci200227u>
- Wallace AC, Laskowski RA, Thornton JM (1995) LIGPLOT: a program to generate schematic diagrams of protein-ligand interactions. *Protein Eng Des Sel* 8:127–134. <https://doi.org/10.1093/protein/8.2.127>